

LMC S154: the first Magellanic symbiotic recurrent nova [★]

Krystian Iłkiewicz¹, Joanna Mikołajewska¹, Brent Miszalski^{2,3}, Mariusz Gromadzki⁴, Berto Monard⁵, and Pía Amigo⁶

¹ Nicolaus Copernicus Astronomical Center, Polish Academy of Sciences, Bartycka 18, 00716 Warsaw, Poland

² South African Astronomical Observatory, PO Box 9, Observatory, 7935, South Africa

³ Southern African Large Telescope Foundation, PO Box 9, Observatory, 7935, South Africa

⁴ Warsaw University Observatory, Al. Ujazdowskie 4, 00-478 Warszawa, Poland

⁵ Kleinkaroo Observatory, Calitzdorp, Western Cape, South Africa

⁶ Instituto de Física, Pontificia Universidad Católica de Valparaíso, Casilla 4059, Valparaíso, Chile

Received ... / Accepted ...

ABSTRACT

Classical nova outburst has been suggested for a number of extragalactic symbiotic stars, but in none of the systems has it been proven. In this work we study the nature of one of these systems, LMC S154. We gathered archival photometric observations in order to determine the timescales and nature of variability in this system. Additionally we carried out photometric and spectroscopic monitoring of the system and fitted synthetic spectra to the observations. Carbon abundance in the photosphere of the red giant is significantly higher than that derived for the nebula, which confirms pollution of the circumbinary material by the ejecta from nova outburst. The photometric and spectroscopic data show that the system reached quiescence in 2009, which means that for the first time all of the phases of a nova outburst were observed in an extragalactic symbiotic star. The data indicate that most probably there were three outbursts observed in LMC S154, which would make this system a member of a rare class of symbiotic recurrent novae. The recurrent nature of the system is supported by the discovery of coronal lines in the spectra, which are observed only in symbiotic stars with massive white dwarfs and with short-recurrence-time outbursts. Gathered evidence is sufficient to classify LMC S154 as the first bona fide extragalactic symbiotic nova, which is likely a recurrent nova. It is also the first nova with a carbon-rich donor.

Key words. binaries: symbiotic – stars: individual: LHA 120-S 154 – novae, cataclysmic variables

1. Introduction

Symbiotic stars (SySts) are interacting binaries with orbital periods ranging from hundreds of days to decades (Gromadzki et al. 2009, 2013). In these systems matter is transferred from a red giant (RG) to a compact companion, typically a white dwarf (WD). The matter could be transferred through a Roche-lobe overflow or wind accretion. Symbiotic stars are classified as D-type (*dust*) systems when the mass donor is a Mira embedded in a dense nebula. In S-type (*stellar*) systems there is a normal RG as a mass donor (see Mikołajewska 2012 for a recent review).

Symbiotic novae (SyNe) are SySts in which the WD has experienced a thermonuclear explosion on its surface. They form a small subclass of classical novae and are very rare among SySts. There are two kinds of SyNe. In typical SyNe the outburst occurs on a medium-mass WD and is relatively quiet. In the case of a massive WD accreting at a high rate the outburst is faster and has a higher amplitude. These outbursts are typically observed more than once, hence they are classified as symbiotic recurrent novae (SyRNe). Thus far, only four SyRNe have been identified (T CrB, V745 Sco, V3890 Sgr and RS Oph), which makes this class of systems extremely rare. A recent review of the outburst activity of SySts is presented in Mikołajewska (2010).

Nine SySts have been discovered in the Large Magellanic Cloud (LMC) and several dozen SySts were discovered outside of the Milky Way in general (Belczyński et al. 2000;

Gonçalves et al. 2008; Kniazev et al. 2009; Miszalski et al. 2014; Mikołajewska et al. 2014; Hajduk et al. 2015; Iłkiewicz & Mikołajewska 2017; Iłkiewicz et al. 2018a,b). Outbursts of Z And-type, which are thought to be caused by increased mass transfer onto a WD, have only been observed in the cases of two extragalactic SySts: LIN 9 (Miszalski et al. 2014) and LHA 120-S 63=LMC S63 (Iłkiewicz et al. 2015). Classical nova outburst has not been proven for any of the extragalactic SySts.

LMC S154 = LHA 120-S 154 = NSV 16200 was an X-ray source located in the LMC observed during a High-Energy Astronomy Observatory (HEAO) 1 survey (Wood et al. 1984) between August 15 1977, and February 15 1978. Remillard et al. (1992) failed to detect the object in EXOSITE satellite observations from October 1984. LMC S154 has not been detected in X-rays since that time. Remillard et al. (1992) carried out optical observations of the object. The observations carried out during the period from February 2 1984, to February 21 1988, showed that the spectrum of the object was characterized by a flat continuum, strong Balmer-series emission lines, and the presence of some low-excitation emission lines. In observations from December 16 1988, LMC S154 showed a changed spectrum characterized by high-excitation emission lines typical for a SySt. Photometric observations of Remillard et al. (1992) showed variability with an amplitude of ~4 mag on a timescale of decades.

The variability of LMC S154 resembles that of SyNe such as for example RX Pup and PU Vul (Remillard et al. 1992; Vogel & Morgan 1994). Vogel & Morgan (1994) measured overabundance of nitrogen in the nebula around the system, which

Send offprint requests to: K. Iłkiewicz, e-mail: ilkiewicz@camk.edu.pl

[★] Based on observations made with the Southern African Large Telescope (SALT) under programme 2015-2-SCI-036

Table 1. The log of spectroscopic observations.

Date	MJD	Telescope	Exposure [s]
2005-11-19	53693	SAAO 1.9m	3x1800
2006-10-07	54015	SAAO 1.9m	3x1800
2007-10-20	54393	SAAO 1.9m	3x1200
2008-10-31	54770	SAAO 1.9m	3x1200
2009-10-31	55135	SAAO 1.9m	3x1200
2015-10-28	57323	SALT	2x60,2x1800

supports classical nova outburst in the recent history of the system. Muerset et al. (1996) detected a C-rich giant in the spectrum of LMC S154 for the first time, which proves the symbiotic nature of the system. The authors derived the spectral type of the cool component to C2,2. Mikołajewska (2004), on the other hand, suggested that the system was of D-type. The SyN nature of the system has had not yet been confirmed, mainly because of a significant gap in photometric observations published by Remillard et al. (1992) ranging from the 1950s to 1980s that hinders estimates of the timescale of its variability. Moreover, the system has not yet been observed in quiescence.

In this work we study **the possible evidence for** the nova outburst of LMC S154. We present results of our spectroscopic and photometric survey supplemented with collected archival observations in Sect. 2. The timescale of outburst(s) activity of the system is analyzed in Sect. 3.1. The discovery of coronal lines in the system is discussed in Sect. 3.2. The variability during quiescence is investigated in Sect. 3.4. The physical parameters **of the cool component** are studied in Sect. 4. The evolution of WD parameters during the most recent outburst is presented in Sect. 5. Arguments supporting the SyN nature of the system are presented in Sect. 6.

2. Observations

2.1. Spectroscopy

We carried out spectroscopic monitoring of LMC S154 using the 1.9-m telescope at the South African Astronomical Observatory (SAAO). The telescope was mounted with the SITe (Scientific Imaging Technologies, INC.) CCD together with a grating spectrograph. The instrumental setup included grating #7 with 300 lines per millimeter and a slit width of 1.5". The resulting resolving power was $R \approx 1000$. The covered spectral range varied with every observation, but approximately covered a range of 3800–7700 Å.

Another low-resolution spectrum was carried out with the Southern African Large Telescope (SALT; Buckley et al. 2006; O'Donoghue et al. 2006) equipped with the Robert Stobie Spectrograph (RSS; Burgh et al. 2003; Kobulnicky et al. 2003) and PG900 grating. Observations were obtained under programme 2015-2-SCI-036 (PI: Mikołajewska). LMC S154 was observed in two wavelength ranges giving the combined covered wavelength range of ~ 3900 –8250 Å.

The spectra obtained using SALT and SAAO 1.9-m telescopes were reduced using the standard IRAF procedures. Spectra were flux-calibrated using spectrophotometric standards. Due to slit losses in SAAO 1.9-m data, as well as the variable pupil design of SALT precluding absolute spectrophotometric calibration, we scaled the flux scale of our spectra to the known V-band photometry near the epoch of observation. The list of spectroscopic observations is presented in Table 1. The spectra are presented in Fig. 1.

We measured fluxes of emission lines by fitting a Gaussian profile. In the case of lines that could not be fitted by a Gaussian profile we integrated the flux above the local continuum. The main source of uncertainty was choosing the local continuum level. Typical uncertainty was of the order of 15% in the case of the strongest lines, and 30% in the case of weakest. The measurements are presented in Table 2 and Fig. 2.

Additionally we employed two International Ultraviolet Explorer (IUE) spectra. The spectra were sp40907 carried out February 2 1991 and sp47766 carried out May 29 1993. The spectra are presented in Fig. 3.

2.2. Photometry

Photometric monitoring of LMC S154 was carried out with a 35-cm Meade RCX400 telescope at the Kleinkaroo Observatory. The instrumental setup included the SBIG ST8-XME CCD camera and V and Ic filters. Observations from each night were reduced and stacked in a standard fashion. The photometry was carried out with the single image mode of the AIP4 image-processing software. The accuracy of the derived magnitudes is better than 0.1 mag.

Additionally we observed LMC S154 in V filter with a 2.5-m Irene du Pont telescope SIT e2K-1 camera at the Las Campanas observatory. Data reduction was performed using standard procedures in IRAF. We employed the brightest stars in the field with magnitudes from the Southern Proper Motion program (SPM4; Girard et al. 2011) as standard stars.

We supplemented our photometry with collected photometric observations from the literature. The magnitudes are presented in Table A.1, Fig. 4, and Fig. 5.

We retrieved publicly available UV images containing LMC S154 taken by the Swift UV optical telescope (UVOT; Gehrels et al. 2004) from the UK Swift Science Data Centre (UKSSDC).¹ Observations were available only in the UV filter UVM2 centered at $\lambda 2246$ Å (see Poole et al. 2008). We followed the UVOT data analysis guide of the UKSSDC to perform aperture photometry on the images using the *heasoft*-6.18 software² and the latest *caldb* files for Swift. Optimal aperture sizes were chosen based on the filter and pixel binning according to Poole et al. (2008). Each image was inspected before calculating the magnitudes to ensure the correct object was in the defined aperture. Table A.2 gives a log of the observations where the magnitudes are provided in the Vega system. The data are presented in Fig. 4.

3. Results

3.1. Timescale of outburst(s)

There is a substantial gap in the photometric observations presented by Remillard et al. (1992). The gap ranges from the 1950s to the 1980s which hinders the determination of whether the **active phases of LMC S154 in the 1940s and 1980s is the same outburst or a two separate events**. The archival observations presented in Table A.1 show that in 1975–1976 LMC S154 was at $m_{pg} \approx 14.8$ mag. This corresponds to the magnitude during an active phase of the system (Remillard et al. 1992), hence the last observed active phase started in the 1970s at the latest.

Interestingly, the spectrum of LMC S154 obtained by Lindsay & Mullan (1963) revealed [O III] lines and no contin-

¹ <http://www.swift.ac.uk/index.php>

² <http://heasarc.gsfc.nasa.gov/heasoft>

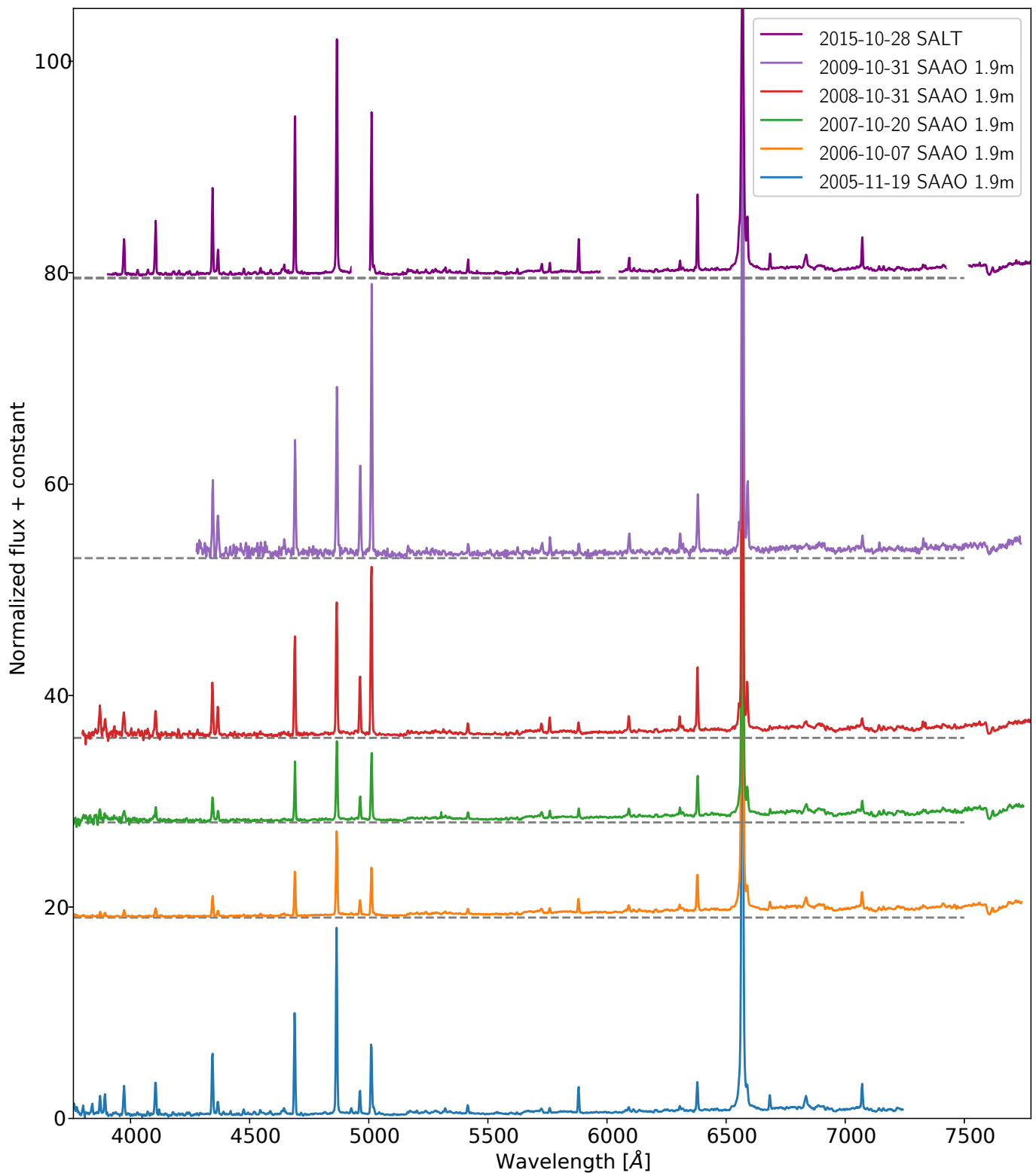


Fig. 1. Spectral variability of LMC S154. The spectra have been normalized in wavelength range 6700–6800Å.

uum. While Lindsay & Mullan (1963) did not give a date for the observation, most of the data collected for their survey were collected in two seasons in 1956 and 1960 (McFarland et al. 1975), at the beginning of the gap in photometric observations. The presence of [O III] in the 1950s, and the similarity of spectra observed by Lindsay & Mullan (1963) and Remillard et al. (1992),

suggest that Lindsay & Mullan (1963) observed LMC S154 at the nebular phase at the end of outburst, and there were at least two outbursts recorded in the history of LMC S154, one with a maximum in the 1940s-50s and the second with a maximum in the 1970s-80s. This makes LMC S154 a member of a rare class of SyRNe. Moreover, in the 1890s, despite the scarcity

Table 2. Observed wavelength from SALT spectrum and relative fluxes of emission lines.

	Date	2005	2006	2007	2008	2009	2015
	MJD	53693	54015	54393	54770	55135	57323
ID	$\lambda_{\text{observed}} [\text{\AA}]$	$100 \times \text{Flux} / \text{Flux}(\text{H}\beta)$					
[Ne III] 3869	3871.04	10	5		26		
H δ , He I	3892.73	12	5		17		
H ϵ	3971.61	17	8		20		15
H δ	4104.50	20	10	15	20		21
H γ	4343.67	35	24	31	40	39	33
[O III] 4363	4366.14	8	7	12	21	31	11
He II 4686	4689.46	54	51	61	76	66	59
H β	4865.15	100	100	100	100	100	100
[O III] 4959	4962.98	12	17	26	42	52	
[O III] 5007	5010.90	41	55	83	130	152	60
He II 5412	5416.11	5	7	8	9	6	5
[N II] 5755	5759.26		6	7	11	9	3
He I 5876	5880.54	13	16	10	8	7	11
[Fe VII] 6086	6091.67		8	11	12	12	5
[O I] 6300	6305.21			6	11	11	3
[Fe X] 6375	6379.89	16	46	49	48	34	28
H α + [N II] 6548	6568.66	661	1012	1000	616	536	
[N II] 6584	6589.26	9	21	29	34	46	31
He I 6678	6683.70	8	8	5			6
O VI 6825	6835.45	15	19	19			10
He I 7065	7070.96	15	18	12			10
[Fe XI] 7892	7897.56						7
	V* [mag]	15.60	15.95	15.90	16.40	16.60	16.35
	Flux (H β) [10^{-13} erg s $^{-1}$ cm $^{-2}$]	3.8	3.6	2.1	1.5	4.4	2.36

Notes: * Assumed magnitude used for scaling of the spectra.

of observations, it seems that the star experienced a drop from $m_{\text{pg}} \approx 14$ mag, a value similar to the one observed at the nova maximum, to $m_{\text{pg}} \approx 17$ mag observed in quiescence (Fig. 5). Therefore it is likely that a drop from maximum of an even older nova outburst was observed at the end of the nineteenth century.

In 2009 the system stopped fading and now shows similar B magnitude to that seen in the 1910s (Fig. 5). This means that the system finally reached quiescence and the outburst that started in 1970s lasted at least ~ 40 years. The $\text{H}\alpha/\text{H}\beta$ ratio was gradually decreasing in the observations of Remillard et al. (1992), while LMC S154 was going out of outburst, and the $\text{H}\alpha/\text{H}\beta$ ratio on all of our spectra is in agreement with the latest spectra of Remillard et al. (1992). This supports the idea that Remillard et al. (1992) observed the start of the transition to quiescence. The ~ 40 -year timescale of outburst is consistent with approximately two outbursts per century. This also implies a period of ~ 10 -20 years in quiescence after an outburst. This period is consistent with the observed quiescence in the 1900s and 1910s between two outbursts (Fig. 5).

3.2. Coronal lines

The [Fe VII] 6086, [Fe X] 6375, and [Fe XI] 7892 coronal lines are present in our spectra (see Table 2). [Fe X] and [Fe XI] lines are detected for the first time in LMC S154, while the [Fe VII] 6086 line appears to be present in the archival spectra, but was not discussed by authors (see Fig. 6). The [Fe X] and [Fe XI] coronal lines are very rare in SySt in general (see e.g., Jordan et al. 1996 and Mikołajewska et al. 2014), but are more common in novae during a nebular phase (Williams 2012) and in supersoft X-ray sources (SSXS), where there is stable hydrogen burning on the surface of the WD (e.g., SMC 3; Jordan et al. 1996). Therefore,

the presence of [Fe X] and [Fe XI] lines in SySt is always associated with nuclear reactions on the surface of WDs.

The [Fe X] 6375 line is observed during the SSXS phase of a nova outburst, when nuclear burning is still continuing (MacDonald et al. 1985; Krautter & Williams 1989). Hence, the [Fe X] 6375 line is well correlated with soft X-ray flux, both in SyNe (Shore et al. 2012) and in classical novae (Moro-Martín et al. 2001). Therefore, it is expected that in LMC S154 the X-ray emission should be the strongest in SSXS phase, around the maximum of [Fe X] 6375 in the 2000s. However, the X-ray emission was detected in the 1970s, and it was not present in the 1980s (Remillard et al. 1992). Since a WD can experience only one SSXS phase during an outburst, this indicates that the X-ray emission in the 1970s was not due to the SSXS phase, but originated in a shock produced by an expanding blast wave (Sokoloski et al. 2006; Drake et al. 2009). This mechanism of radiation is expected at the earliest phase of the nova outburst is therefore a strong argument in support of the idea that the most recent outburst started in the 1970s.

Assuming a distance to LMC of 49.97 kpc (Pietrzyński et al. 2013) a reddening $E(B - V) = 0.17$ mag (Muerset et al. 1996) and using [Fe X] 6375 flux from the 2015 SALT spectrum we get $L([\text{Fe X}] 6375) = 2.0 \times 10^{34}$ erg s $^{-1}$. Maximum [Fe X] 6375 flux observed during the last outburst of RS Oph was 1.5×10^{-10} erg cm $^{-2}$ s $^{-1}$ (Iijima 2009). Assuming a distance to RS Oph of 1.4 kpc (Barry et al. 2008) and reddening $E(B - V) = 0.69$ mag (Zamanov et al. 2018) this corresponds to a luminosity $L([\text{Fe X}] 6375) = 1.9 \times 10^{35}$ erg s $^{-1}$. In SMC 3, an SSXS SySt, the [Fe X] 6375 line was 2.0×10^{-14} erg cm $^{-2}$ s $^{-1}$ (Morgan 1992) which after scaling for reddening $E(B - V) = 0.099$ mag (Hilditch et al. 2005) and SMC distance of 60.6 kpc (Hilditch et al. 2005) gives

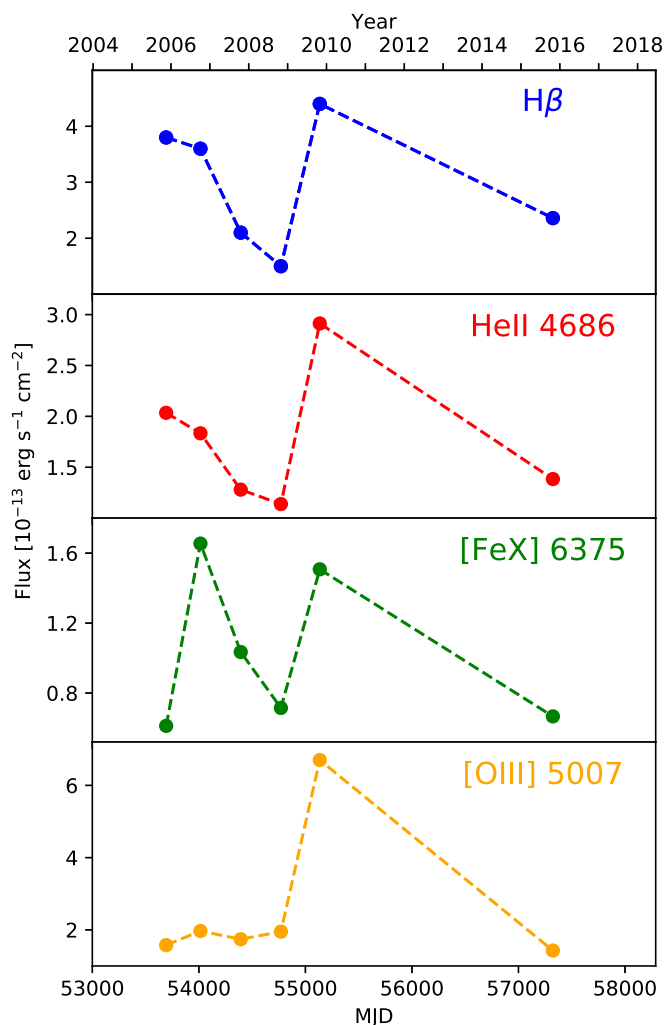


Fig. 2. Variability of emission line fluxes in LMC S154.

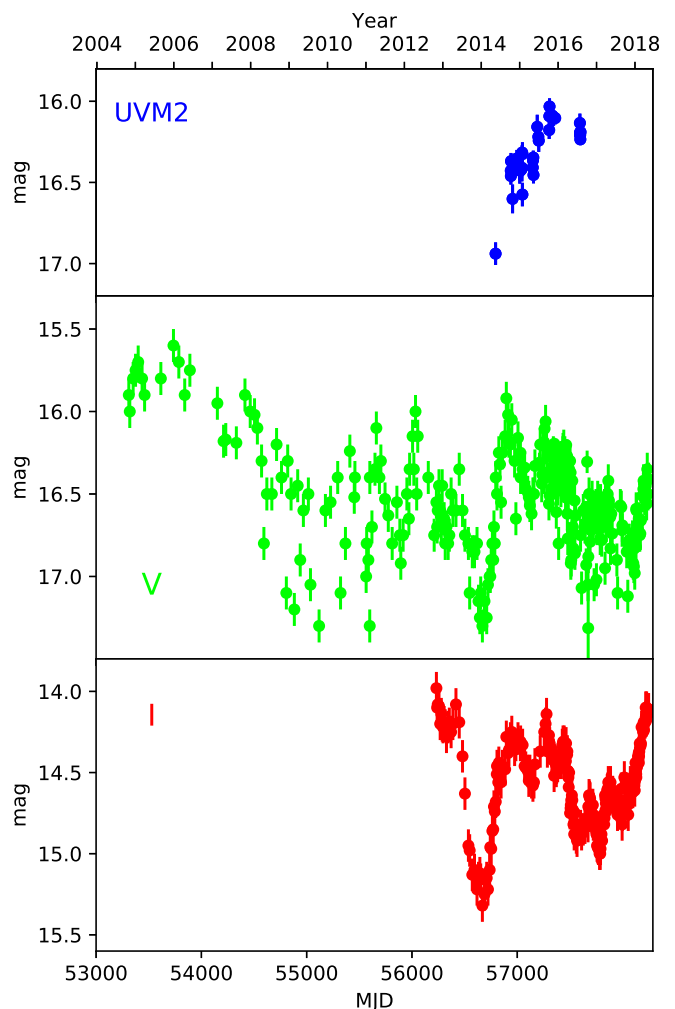


Fig. 4. Most recent photometric variability of LMC S154.

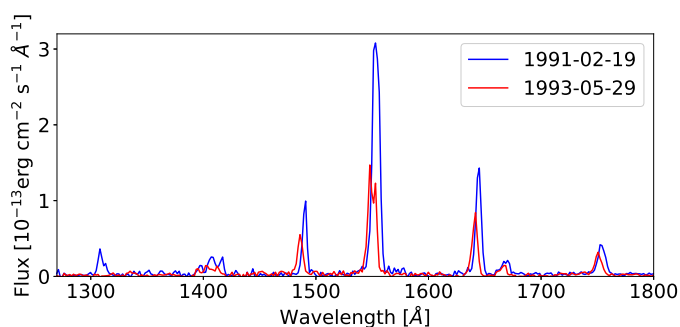


Fig. 3. IUE spectra of LMC S154.

$L([\text{Fe x}] 6375) = 1.1 \times 10^{34} \text{ erg s}^{-1}$. Given the differences in metallicity and reddening of these objects, one could say that the luminosity of the $[\text{Fe x}]$ line in the two X-ray-bright objects is consistent with $[\text{Fe x}]$ luminosity in LMC S154. This confirms that $[\text{Fe x}]$ and $[\text{Fe xi}]$ emission lines are due to the SSXS phase of outburst.

Given the spectroscopic evolution of LMC S154 in observations of Remillard et al. (1992) the maximum of the nova outburst was most probably no later than their first spectroscopic observation in February 1984. The maximum was probably even earlier given the fact that the star was detected in X-rays in the

1970s. The coronal lines were not present at least until May 1993 (Muerstet et al. 1996) which corresponds to at least 9 years after the maximum. The first spectrum with the $[\text{Fe x}] 6375$ line detected was from 2005, at least 21 years after the maximum. The emission line was still present more than 31 years after the maximum.

Detection of this line so late after outburst is somewhat surprising. Typically in the recurrent novae and SyRNe the $[\text{Fe x}] 6375$ line is detected ~ 1 month after outburst (see e.g., Williams et al. 1991; Iijima 2009) while in classical novae this line can be detected a few years after the maximum (Krautter & Williams 1989). Moreover, in SyNe the $[\text{Fe x}] 6375$ line is observed only in the case of massive WDs that exhibit nova outburst on short timescales; for example in RS Oph (Osborne et al. 2011), V407 Cyg (Shore et al. 2012), and T CrB (Bloch & Mao-Lin 1953). In SyNe, with long timescales and less massive WDs, only $[\text{Fe vii}]$ lines are observed; for example in RX Pup (Mikolajewska et al. 1999), AG Peg (Kenyon et al. 2001), and PU Vul (Yoo 2007). This suggests that the outburst timescale in LMC S154 was in intermediate range ($\ll 100$ yrs) which is consistent with the hypothesis that there were two separate outbursts, one with its maximum in the 1940s-50s and the second with its maximum in the 1970s-80s.

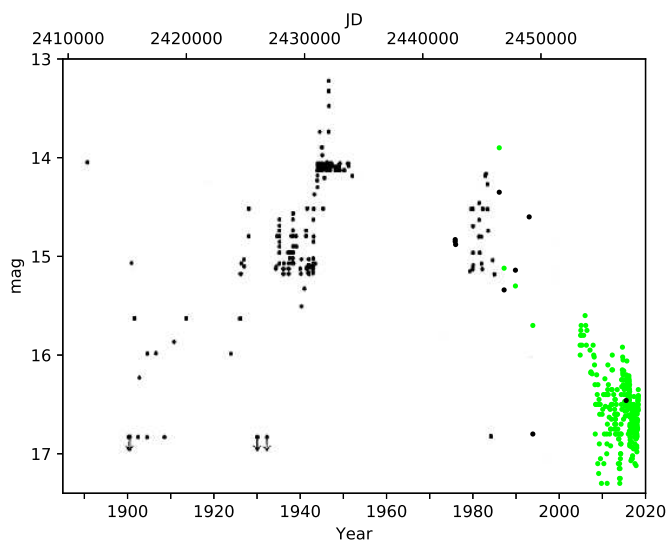


Fig. 5. Historical light curve of LMC S154. The black points are magnitudes in m_{pg} and B filters. The green points are magnitudes in V filter.

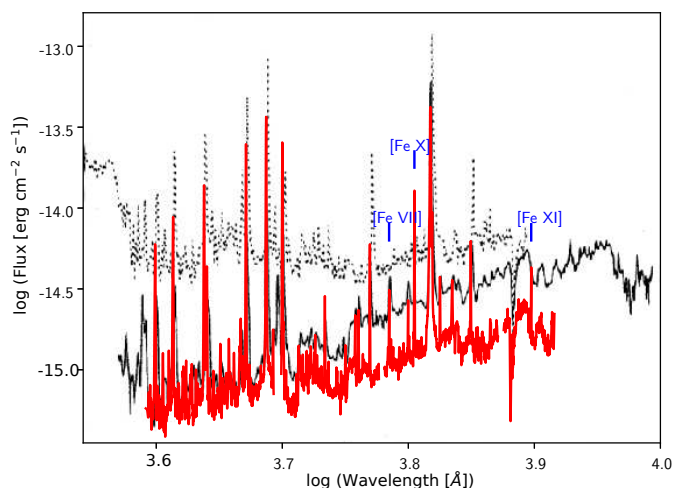


Fig. 6. Comparison of the most recent SALT spectrum of LMC S154 from 2015 (red line) to the spectra obtained by Remillard et al. (1992) in 1989 (black dashed line) and Muerset et al. (1996) in 1993 (black solid line).

3.3. X-ray and UV emission during outburst

X-ray radiation was detected in LMC S154 between August 15 1977 and February 2 1978 and has not been detected since (Remillard et al. 1992). If there was in fact a nova outburst in the system that came to a halt in the 1990s, the subsequent lack of X-ray radiation is expected. In order to confirm the reality of X-ray radiation in LMC S154 during the outburst we search the High Energy Astrophysics Science Archive Research Center³ (HEASARC) for additional reported observations. The only finding is the reported detection of LMC S154 by the Eighth Orbiting Solar Observatory (OSO-8) on October 14 1975. The source was detected at 4.7 ± 0.1 counts s^{-1} in the range of 2–60 keV. This observation was before the one reported by (Remillard et al. 1992) and supports the reality of X-ray emission from LMC S154 during the most recent outburst.

³ <http://heasarc.nasa.gov/>

Change of emission line fluxes in the two IUE spectra is evident (Fig. 3). Fluxes of all of detected emission lines decreased between 1991 and 1993. This is consistent with the drop in brightness of the system during 1993 (Table A.1). In the spectrum from 1993 the emission lines appear to be narrower. This lead to the separation of C iv 1548 and C iv 1551 lines. A similar drop in the width of emission lines after a nova outburst was observed for example in AG Peg (Kenyon et al. 1993). This is probably related to the fact that these lines are formed in the wind of the WD, which has slowed down after the outburst. Interestingly there is an apparent blueshift of the emission lines in the spectrum from 1993.

3.4. Photometric and spectroscopic variability in quiescence

The outburst of LMC S154 ended in 2009 and the star stopped fading. After the end of the outburst, during 2013 and 2014, LMC S154 showed a dip in its light curve, where the brightness decreased by ~ 1 mag in V and I bands (Fig. 4). After recovery from the dip the Swift light curve showed that the star brightened by ~ 1 mag in 1.5 yr (Fig. 4). Similar behavior was observed in V band in RX Pup, where both the dip at the end of the outburst and a subsequent brightening were observed (Mikolajewska et al. 1999). This was interpreted as a signature of ceasing of the hot component wind which allowed for a start of accretion of the cool component wind (Mikolajewska et al. 1999; Mikolajewska et al. 2002). Another explanation of brightening in the Swift UV observations could be active phases observed in other SyRNe (see e.g., Iłkiewicz et al. 2016).

In the most recent observations in V and I bands LMC S154 shows quasi-periodic variability on a timescale of ~ 250 d (Fig. 4). This variability is not present in the Swift $UVM2$ band. The simplest interpretation would be pulsations of the RG. This is consistent with the fact that the system shows variability with an amplitude of ~ 0.5 mag in J and K filters (see Table A.1). Moreover, pulsations would be consistent with the position of the RG on the K versus $(J - K)$ colour–magnitude diagram for LMC (Soszynski et al. 2007).

In the visual spectrum the [N II] emission lines are detected for the first time. They are clearly visible in all of our spectra (Fig. 1). The presence of these lines is typical for a nebular phase after a nova outburst (see e.g., Bode & Evans 2008). Both the [N II] and [O III] nebular lines were roughly constant in the years 2005–2008 (see Fig. 2, Table 2). The fluxes were significantly higher in 2009, which was probably related to the end of the outburst. In the spectrum that followed, carried out in 2015, the forbidden lines had the same flux as during the outburst.

The H and He permitted lines showed a gradual decrease in the years 2005–2008 (Fig. 2, Table 2) similar to the one observed in photometric observations (Fig. 4). In 2009, when the photometric decline had come to a halt, the permitted emission lines showed an increase in flux similar to the one observed in the case of forbidden lines. Moreover, in 2015, both the permitted and emission lines showed similar fluxes to those found at the end of the photometric decline.

In the case of the [Fe x] 6375 emission line the variability is the most complicated. The behavior of this line is similar to the variability seen for H and He permitted lines. The only difference is that the first two of our spectra show an increase in flux which is succeeded by a gradual decrease. This may be related to stopping of the WD wind, which lead to a decrease in the density of the material close to the WD, and allowed for emission of forbidden lines in a high-excitation environment.

Table 3. Parameters of the red giant from analysis of the infrared SED of LMC S154.

Parameters	Best value	Probability [%]
T_{eff}	4000	79.76
L	12300 L_{\odot}	78.29
log g	0	100
Mass	2 M_{\odot}	100
C/O	2	43.15
\dot{M}_{dust}	$1.27 \times 10^{-9} M_{\odot}/\text{yr}$	35.75
R_{in}	4.5 R_{star}	100
$\tau_{11.3}$	0.2	100

Notes. \dot{M}_{dust} – dust mass-loss rate, R_{in} – inner radius of the dust shell, $\tau_{11.3}$ – optical depth at 11.3 microns

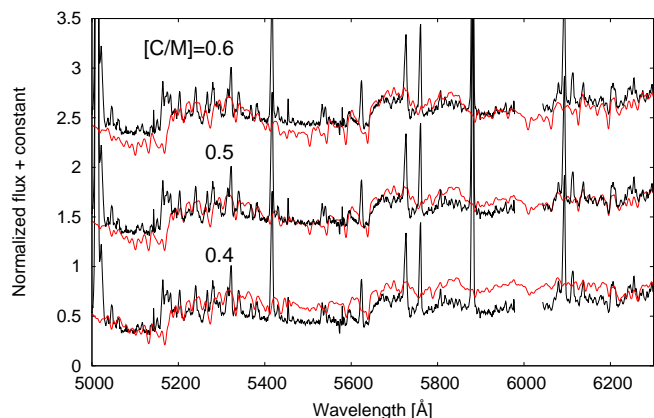
4. Cool component

The cool component of LMC S154 was classified as a C-rich giant by Muerstet et al. (1996). The authors determined its type as C2,2. Nevertheless, thus far the chemical composition of the RG has not been estimated and only the chemical composition of the nebula around the system has been calculated using emission lines (Vogel & Morgan 1994). This gave a consistent overabundance of carbon (C/O=1.19). Nevertheless, the outburst in the history of the system can pollute the nebula with material from the WD and cause the abundances to misrepresent the giant chemical composition (see e.g., Hkiewicz et al. 2015). For this reason we attempted to estimate the carbon abundance in the cool component of LMC S154 by fitting a synthetic spectrum to the observations.

In order to obtain an initial guess for the RG parameters we fitted a GRAMS C-rich grid of models of dust shells around red supergiant and AGB stars (Srinivasan et al. 2011) to the infrared spectral energy distribution (SED) of LMC S154. We employed photometry from 2MASS All-Sky Point Source Catalog (Skrutskie et al. 2006), AKARI/IRC Mid-Infrared All-Sky Survey (Ishihara et al. 2010), and the IRAS Catalog of Point Sources (Helou & Walker 1988). Bayesian analysis of data was performed using the virtual observatory SED analyzer (VOSA) service (Bayo et al. 2008). We assumed $E_{B-V}=0.17$ (Muerstet et al. 1996) and a distance to LMC of $d=49.97$ kpc (Pietrzyński et al. 2013). The caveat is that the models were only for a solar metallicity and in the grid of models there was a highest possible log $g = 0$. The results of our analysis are presented in Table 3.

We calculated synthetic spectra using the SPECTRUM code (Gray & Corbally 1994) and models from Castelli & Kurucz (2004). During calculations we employed the updated Plez (1998) TiO line list from their website⁴ and solar abundances from Grevesse & Sauval (1998). We assumed LMC metallicity $[M/H] = -0.5$ dex and log $g = 0$. Our grid of synthetic spectra consisted of models with $T_{\text{eff}} = 3500\text{--}4500$ K and $[C/M] = 0.0\text{--}1.0$ dex. The results of least square fitting of synthetic spectra to the SALT spectrum of LMC S154 are presented in Fig. 7. Using this procedure we derived $T_{\text{eff}} = 4000 \pm 250$ and $[C/M] = 0.50 \pm 0.05$ dex. Additional uncertainty could be introduced by the presence of a nebular contribution to the continuum, which we did not consider.

After assuming the same oxygen abundance as assumed metallicity from our fit we derive $C/O \approx 1.7$. This value is clearly higher than $C/O=1.19$ derived by Vogel & Morgan (1994) for the nebula, even taking into account the relatively low accuracy


Fig. 7. Fit of synthetic spectra (red lines) to the SALT spectrum of LMC S154 (black lines).

of the Vogel & Morgan (1994) method. This confirms that the nebula has been polluted by the material ejected from the WD during the nova outburst.

5. WD evolution during outburst

During a maximum of both a SyNe and Z-And outburst the WD experiences a ““supergiant phase”, where the WD resembles an A–F supergiant. During this phase most of the light is shifted towards optical bands. Therefore, we can estimate a luminosity of the WD during maximum by measuring the brightness of the system in the optical bands, assuming that the bolometric correction $BC \approx 0$. The maximum m_{pg} observed in the archival outburst was ~ 13.1 mag (Fig. 5). Due to gaps in photometric data we assume this is the maximum magnitude during both outbursts. A lower limit of the maximum magnitude of the 1980s outburst is ~ 14 mag. After correcting for a reddening $E(B-V)=0.17$ mag (Muerstet et al. 1996) and using a distance to LMC of 49.97 kpc (Pietrzyński et al. 2013) this method gives a $L_{\text{WD}} \sim 8300\text{--}23000 L_{\odot}$ during the outburst maximum.

At the beginning of the nebular phase, the luminosity of the WD has been estimated to be $L_{\text{WD}} = 3000 \pm 1000 L_{\odot}$ in May 1993 (Vogel & Morgan 1994; Muerstet et al. 1996) based on UV spectroscopy. Using our data we can estimate WD luminosity with Eq. 8 of Kenyon et al. (1991). Fluxes measured in 2015 (Table 2) after correcting for reddening give $L_{\text{WD}} \sim 4200 L_{\odot}$. Similarly, the O VI 6825 flux from the same spectrum gives $L_{\text{WD}} \sim 4700 L_{\odot}$ using Eq. 8 of Mikolajewska et al. (1997). Both of these estimates have an uncertainty of a factor of two.

While there is no data covering the maximum of the outburst allowing us to estimate WD temperature, Muerstet & Nussbaumer (1994) estimated $T_{\text{hot}} = 140 \pm 15$ based on spectra from 1993. Using our data we can estimate the temperature of the WD using a relation proposed by Muerstet & Nussbaumer (1994):

$$T_{\text{WD}}(\text{kK}) = \chi_{\text{max}}(\text{eV}), \quad (1)$$

where χ_{max} is the highest observed ionization potential. The highest ionization stage observed in LMC S154 is Fe^{+10} , which gives $T_{\text{WD}}=291$ kK.

Evolution of the WD during outburst is presented in Table 4. During the decline from maximum, the temperature of the WD increased by over a factor two. Such a behavior is expected during decline from classical nova outburst, and was observed for example in the SyNe PU Vul (Kato et al. 2012).

⁴ <http://www.pages-perso-bertrand-plez.univ-montp2.fr/>

Table 4. Parameters of the WD during outburst (see text).

Outburst phase	Year	$L_{\text{WD}} [L_{\odot}]$	$T_{\text{WD}} [\text{kK}]$
Maximum	1980's	8300–23000	
Early nebular phase	1993	3000 ± 1000	140 ± 15
Nebular phase	2015	~ 4200	291

6. Symbiotic nova classification

Based on the evolution of the WD parameters during the drop from maximum it is clear that the variability of LMC S154 is due to an outburst. However, a similar low-amplitude outburst could be explained by a Z And-type outburst, and the SyN nature of the system cannot be confirmed by a light curve and WD parameters alone.

We confirm the SyN nature of the object using spectroscopic features detected in the spectrum during nebular phase. LMC S154 shows a rich nebular spectrum, which is not observed in Z And-type stars after outburst. In particular, the [N II] forbidden lines are in strong emission in LMC S154, while in the case of Z And-type outbursts, forbidden lines with such low critical densities are never observed (see e.g., Miszalski et al. 2014 and references therein).

Another strong argument in favor of the classical nova classification is provided by the evolution of the object in X-rays. In LMC S154, X-rays were detected only near the maximum of outburst and have not been detected since then (Remillard et al. 1992). The opposite is expected in the case of Z-And-type outbursts, where the X-ray flux is lowest during outburst and highest during quiescence (Greiner et al. 1997).

7. Conclusions and discussion

While nova outbursts have been suggested for some extragalactic SySts, none have thus far been proven. **This is perhaps mainly due to the fact that observations have never been carried out of all of the phases of an outburst in these systems.** Most notably, in the case of Sanduleak's star, outburst was suggested on the basis of monotonic fading of the star (Angeloni et al. 2014), but the beginning of the outburst was not observed in the history of the star, nor did the star reach quiescence. Moreover, an outburst was suggested in the case of M31SyS J004322.50+413940.9 (Mikołajewska et al. 2014) but was never demonstrated.

In this work we study the possible evidence for the suggested nova outburst in the history of the extragalactic SySt, LMC S154. We gathered archival observations which confirmed that the variability of the system is due to a classical nova outburst. Results of our monitoring in the years 2005–2015 show that the outburst ended in 2009. This means that the star finally reached quiescence and all phases of an outburst were observed. Abundance of carbon in the photosphere of the RG is significantly higher than the abundance derived for the nebula, which confirms pollution of the circumbinary material by the nova ejecta. The luminosity and temperature changes of the WD are consistent with a nova outburst. The available evidence proves that LMC S154 is a bona fide SyN.

The archival data strongly suggest that there has been more than one outburst recorded in the history of LMC S154, which would make this system a member of a rare class of SyRNe. This makes this object the first SyRN in MCs and in general the third recurrent nova in the LMC (see e.g., Mróz et al. 2016). While it is possible that LMC S154 showed only one nova outburst with

one long maximum or more than one shorter maximum, as in the case of RX Pup (Mikołajewska et al. 1999), the SyRNe classification is supported by the detection of [O III] lines between the two observed maxima, in the 1940s and in the 1980s, and the nondetection in the 1980s. These lines are characteristic of the nebular phase of outburst, and once detected they last until the end of outburst, even if more than one maximum of the outburst is present (see e.g., RX Pup). This means that the maxima detected in the 1940s and the 1980s were associated with two different outbursts, and that each of them was followed by a nebular phase. Also in favor of the SyRN nature of LMC S154 is the discovery of [Fe x] and [Fe xi] coronal lines. These lines are rare in SySts, and in SyNe they are observed only during the SSXS phase of nova outbursts on a massive WD. Another argument in favor of the recurrent nature of LMC S154 is provided by the detection of X-ray radiation in the 1980s. The X-ray radiation from LMC S154 most probably originated in a shock produced by an expanding blast wave, which is expected at the earliest phases of an outburst.

LMC S154 is the first classical nova to be discovered with a C-rich donor. While there have been no theoretical studies of nova outbursts with such a C-rich donor, it is clear that the abundance of carbon in the accreted material will have an influence on the evolution of the outburst. Together with the fact that LMC S154 appears to suffer an outburst of a significantly longer timescale compared to other SyRNe (T CrB, V745 Sco, V3890 Sgr and RS Oph), this makes this object an interesting case for the study of nova outbursts.

Acknowledgements. KI has been financed by the Polish Ministry of Science and Higher Education Diamond Grant Programme via grant 0136/DIA/2014/43 and by the Foundation for Polish Science (FNP) within the START program. This study has been partially funded by the National Science Centre, Poland, grant OPUS 2017/27/B/ST9/01940. Polish participation in SALT is funded by grant No. MNiSW DIR/WK/2016/07. We acknowledge with thanks the variable star observations from the AAVSO International Database contributed by observers worldwide and used in this research. This research has made use of data and/or software provided by the High Energy Astrophysics Science Archive Research Center (HEASARC), which is a service of the Astrophysics Science Division at NASA/GSFC and the High Energy Astrophysics Division of the Smithsonian Astrophysical Observatory. This research has made use of the VizieR catalogue access tool, CDS, Strasbourg, France. This publication makes use of VOSA, developed under the Spanish Virtual Observatory project supported from the Spanish MICINN through grant AyA2011-24052.

References

- Angeloni, R., Ferreira Lopes, C. E., Masetti, N., et al. 2014, *MNRAS*, 438, 35
- Barry, R. K., Mukai, K., Sokoloski, J. L., et al. 2008, in *Astronomical Society of the Pacific Conference Series*, Vol. 401, RS Ophiuchi (2006) and the Recurrent Nova Phenomenon, ed. A. Evans, M. F. Bode, T. J. O'Brien, & M. J. Darnley, 52
- Bayo, A., Rodrigo, C., Barrado Y Navascués, D., et al. 2008, *A&A*, 492, 277
- Belczyński, K., Mikołajewska, J., Munari, U., Ivison, R. J., & Friedjung, M. 2000, *A&AS*, 146, 407
- Bloch, M. & Mao-Lin, T. 1953, *Annales d'Astrophysique*, 16, 73
- Bode, M. F. & Evans, A. 2008, *Classical Novae*
- Buckley, D. A. H., Burgh, E. B., Cottrell, P. L., et al. 2006, in *Proc. SPIE*, Vol. 6269, Society of Photo-Optical Instrumentation Engineers (SPIE) Conference Series, 62690A
- Burgh, E. B., Nordsieck, K. H., Kobulnicky, H. A., et al. 2003, in *Proc. SPIE*, Vol. 4841, Instrument Design and Performance for Optical/Infrared Ground-based Telescopes, ed. M. Iye & A. F. M. Moorwood, 1463–1471
- Castelli, F. & Kurucz, R. L. 2004, *ArXiv Astrophysics e-prints* [astro-ph/0405087]
- Cioni, M.-R., Loup, C., Habing, H. J., et al. 2000, *A&AS*, 144, 235
- Drake, J. J., Laming, J. M., Ness, J.-U., et al. 2009, *ApJ*, 691, 418
- Gehrels, N., Chincarini, G., Giommi, P., et al. 2004, *ApJ*, 611, 1005
- Giménez, A., Mas-Hesse, J. M., Domingo, A., & Omc Consortium. 2001, in *ESA Special Publication*, Vol. 459, Exploring the Gamma-Ray Universe, ed. A. Gimenez, V. Reglero, & C. Winkler, 375–381

- Girard, T. M., van Altena, W. F., Zacharias, N., et al. 2011, *AJ*, 142, 15
- Gonçalves, D. R., Magrini, L., Munari, U., Corradi, R. L. M., & Costa, R. D. D. 2008, *MNRAS*, 391, L84
- Gray, R. O. & Corbally, C. J. 1994, *AJ*, 107, 742
- Greiner, J., Bickert, K., Luthardt, R., et al. 1997, *A&A*, 322, 576
- Grevesse, N. & Sauval, A. J. 1998, *Space Sci. Rev.*, 85, 161
- Gromadzki, M., Mikołajewska, J., & Soszyński, I. 2013, *Acta Astron.*, 63, 405
- Gromadzki, M., Mikołajewska, J., Whitelock, P., & Marang, F. 2009, *Acta Astron.*, 59, 169
- Hajduk, M., Gromadzki, M., Mikołajewska, J., Miszalski, B., & Soszyński, I. 2015, *Acta Astron.*, 65, 139
- Hambly, N. C., Irwin, M. J., & MacGillivray, H. T. 2001, *MNRAS*, 326, 1295
- Helou, G. & Walker, D. W., eds. 1988, *Infrared astronomical satellite (IRAS) catalogs and atlases. Volume 7: The small scale structure catalog, Vol. 7, 1–265*
- Hilditch, R. W., Howarth, I. D., & Harries, T. J. 2005, *MNRAS*, 357, 304
- Iijima, T. 2009, *A&A*, 505, 287
- Hkiewicz, K. & Mikołajewska, J. 2017, *A&A*, 606, A110
- Hkiewicz, K., Mikołajewska, J., Miszalski, B., Gromadzki, M., & Whitelock, P. A. 2015, *MNRAS*, 451, 3909
- Hkiewicz, K., Mikołajewska, J., Miszalski, B., Kozłowski, S., & Udalski, A. 2018a, *MNRAS*, 476, 2605
- Hkiewicz, K., Mikołajewska, J., Shara, M. M., et al. 2018b, *ArXiv e-prints [arXiv:1811.06696]*
- Hkiewicz, K., Mikołajewska, J., Stoyanov, K., Manousakis, A., & Miszalski, B. 2016, *MNRAS*, 462, 2695
- Ishihara, D., Onaka, T., Kataza, H., et al. 2010, *A&A*, 514, A1
- Jordan, S., Schmutz, W., Wolff, B., Werner, K., & Muerset, U. 1996, *A&A*, 312, 897
- Kato, M., Mikołajewska, J., & Hachisu, I. 2012, *ApJ*, 750, 5
- Kenyon, S. J., Mikołajewska, J., Mikołajewski, M., Polidan, R. S., & Slovak, M. H. 1993, *AJ*, 106, 1573
- Kenyon, S. J., Oliverson, N. A., Mikołajewska, J., et al. 1991, *AJ*, 101, 637
- Kenyon, S. J., Proga, D., & Keyes, C. D. 2001, *AJ*, 122, 349
- Kniazev, A. Y., Väisänen, P., Whitelock, P. A., et al. 2009, *MNRAS*, 395, 1121
- Kobulnicky, H. A., Nordsieck, K. H., Burgh, E. B., et al. 2003, in *Proc. SPIE, Vol. 4841, Instrument Design and Performance for Optical/Infrared Ground-based Telescopes*, ed. M. Iye & A. F. M. Moorwood, 1634–1644
- Krautter, J. & Williams, R. E. 1989, *ApJ*, 341, 968
- Lindsay, E. M. & Mullan, D. J. 1963, *Irish Astronomical Journal*, 6, 51
- MacDonald, J., Fujimoto, M. Y., & Truran, J. W. 1985, *ApJ*, 294, 263
- McFarland, J., Lindsay, E. M., & Andrews, A. D. 1975, *Atlas for the Armagh survey of h-alpha emission objects in the Large Magellanic Cloud*
- Mikołajewska, J. 2004, in *Revista Mexicana de Astronomía y Astrofísica*, vol. 27, Vol. 20, *Revista Mexicana de Astronomía y Astrofísica Conference Series*, ed. G. Tovmassian & E. Sion, 33–34
- Mikołajewska, J. 2010, *ArXiv e-prints [arXiv:1011.5657]*
- Mikołajewska, J. 2012, *Baltic Astronomy*, 21, 5
- Mikołajewska, J., Acker, A., & Stenholm, B. 1997, *A&A*, 327, 191
- Mikołajewska, J., Brandi, E., Garcia, L., et al. 2002, in *American Institute of Physics Conference Series, Vol. 637, Classical Nova Explosions*, ed. M. Hernandez & J. José, 42–46
- Mikołajewska, J., Brandi, E., Hack, W., et al. 1999, *MNRAS*, 305, 190
- Mikołajewska, J., Caldwell, N., & Shara, M. M. 2014, *MNRAS*, 444, 586
- Miszalski, B., Mikołajewska, J., & Udalski, A. 2014, *MNRAS*, 444, L11
- Monet, D. G., Dahn, C. C., Vrba, F. J., et al. 1992, *AJ*, 103, 638
- Monet, D. G., Levine, S. E., Canzian, B., et al. 2003, *AJ*, 125, 984
- Morgan, D. H. 1992, *MNRAS*, 258, 639
- Moro-Martín, A., Garnavich, P. M., & Noriega-Crespo, A. 2001, *AJ*, 121, 1636
- Morrison, J. E., Röser, S., McLean, B., Bucciarelli, B., & Lasker, B. 2001, *AJ*, 121, 1752
- Mróz, P., Udalski, A., Poleski, R., et al. 2016, *ApJS*, 222, 9
- Muerset, U., Schild, H., & Vogel, M. 1996, *A&A*, 307, 516
- Muerset, U. & Nussbaumer, H. 1994, *A&A*, 282, 586
- O'Donoghue, D., Buckley, D. A. H., Balona, L. A., et al. 2006, *MNRAS*, 372, 151
- Osborne, J. P., Page, K. L., Beardmore, A. P., et al. 2011, *ApJ*, 727, 124
- Pietrzyński, G., Graczyk, D., Gieren, W., et al. 2013, *Nature*, 495, 76
- Plez, B. 1998, *A&A*, 337, 495
- Poole, T. S., Breueveld, A. A., Page, M. J., et al. 2008, *MNRAS*, 383, 627
- Remillard, R. A., Rosenthal, E., Tuohy, I. R., et al. 1992, *ApJ*, 396, 668
- Shore, S. N., Wahlgren, G. M., Augusteijn, T., et al. 2012, *A&A*, 540, A55
- Skrutskie, M. F., Cutri, R. M., Stiening, R., et al. 2006, *AJ*, 131, 1163
- Sokoloski, J. L., Luna, G. J. M., Mukai, K., & Kenyon, S. J. 2006, *Nature*, 442, 276
- Soszyński, I., Dziembowski, W. A., Udalski, A., et al. 2007, *Acta Astron.*, 57, 201
- Srinivasan, S., Sargent, B. A., & Meixner, M. 2011, *A&A*, 532, A54
- Vogel, M. & Morgan, D. H. 1994, *A&A*, 288
- Williams, R. 2012, *The Astronomical Journal*, 144, 98
- Williams, R. E., Hamuy, M., Phillips, M. M., et al. 1991, *ApJ*, 376, 721
- Wood, K. S., Meekins, J. F., Yentis, D. J., et al. 1984, *ApJS*, 56, 507
- Yoo, K.-H. 2007, *Journal of Korean Astronomical Society*, 40, 39
- Zamanov, R. K., Boeva, S., Latev, G. Y., et al. 2018, *MNRAS*, 480, 1363

Appendix A: Photometric data

Table A.1. Photometric observations of LMC S154.

Date	JD -2400000	m_{pg} / B [mag]	V [mag]	R [mag]	I / I_c [mag]	J [mag]	K [mag]	Ref.
1975-11-28	42744	14.85						1
1975-11-29	42745	14.83±0.4						2
1976-01-04	42781	14.88±0.4						2
1982-05-07	45096	14.6		12.5				3
1982-11				12.95				4
1982-11		14.72		13.52	13.02			4
1986-02-11	46472	14.35	13.90	13.28				5
1987-03-28	46882	15.34	15.12					5
1989-11-11	47841	15.14	15.30	13.65				5
1993-11-22	49313	16.8	15.7	14.2				6
1997-03-02	50509				14.25±0.03	12.18±0.06	9.64±0.08	7
1998-10-25	51111				13.69±0.04	11.5±0.06	9.13±0.10	7
1998-11-23	51140				13.74±0.03	11.72±0.06	9.40±0.06	7
1998-12-02	51149					11.71±0.03	9.38±0.02	8
2004-11-01	53311		15.9±0.1					9
2004-11-10	53320		16.0±0.1					9
2004-12-12	53352		15.8±0.1					9
2005-01-04	53375		15.75±0.1					9
2005-01-29	53400		15.7±0.1					9
2005-03-07	53437		15.8±0.1					9
2005-03-31	53461		15.9±0.1					9
2005-09-02	53615		15.8±0.1					9
2005-12-30	53735		15.6±0.1					9
2006-02-19	53786		15.7±0.1					9
2006-04-16	53842		15.9±0.1					9
2006-06-04	53891		15.75±0.1					9
2007-02-20	54152		15.95±0.1					9
2007-04-20	54211		16.18±0.1					9
2007-05-11	54232		16.17±0.1					9
2007-08-20	54332		16.19±0.1					9
2007-11-09	54414		15.9±0.1					9
2007-12-29	54464		16.0±0.1					9
2008-02-08	54505		16.02±0.1					9
2008-03-06	54532		16.1±0.1					9
2008-04-15	54572		16.3±0.1					9
2008-05-07	54594		16.8±0.1					9
2008-06-04	54622		16.5±0.1					9
2008-07-22	54669		16.5±0.1					9
2008-09-05	54714		16.2±0.1					9
2008-10-22	54761		16.4±0.1					9
2008-12-06	54807		17.1±0.1					9
2008-12-19	54820		16.3±0.1					9
2009-01-20	54852		16.5±0.1					9
2009-02-20	54883		17.2±0.1					9
2009-03-24	54915		16.45±0.1					9
2009-04-17	54939		16.9±0.1					9
2009-05-17	54969		16.6±0.1					9
2009-07-04	55016		16.5±0.1					9
2009-07-24	55036		17.05±0.1					9
2009-10-14	55118		17.3±0.1					9
2009-12-13	55178		16.6±0.1					9
2010-01-30	55227		16.55±0.1					9
2010-04-08	55295		16.4±0.1					9
2010-05-05	55322		17.1±0.1					9
2010-06-11	55358		16.15±0.40					10
2010-06-21	55368		16.8±0.1					9
2010-08-02	55410		16.24±0.1					9
2010-09-13	55452		16.52±0.1					9
2010-09-19	55458		16.4±0.1					9
2011-01-03	55565		17.0±0.1					9

2011-01-08	55570	16.8±0.1		9
2011-01-24	55586	16.9±0.1		9
2011-02-06	55599	17.3±0.1		9
2011-02-06	55599	16.20±0.40		10
2011-02-07	55600	16.4±0.1		9
2011-02-13	55605	16.25±0.65		10
2011-02-16	55608	15.30±0.30		10
2011-02-27	55620	16.7±0.1		9
2011-03-28	55649	16.35±0.1		9
2011-04-10	55662	16.1±0.1		9
2011-05-09	55691	16.4±0.1		9
2011-05-23	55705	16.3±0.1		9
2012-05-31	56078	16.00±0.55		10
2012-06-25	56103	15.70±0.60		10
2011-07-02	55744	16.53±0.1		9
2011-08-02	55775	16.63±0.1		9
2011-09-08	55812	16.8±0.1		9
2011-10-22	55857	16.55±0.1		9
2011-11-19	55885	16.75±0.1		9
2011-11-28	55894	16.92±0.1		9
2011-12-20	55916	16.75±0.1		9
2012-01-25	55952	16.5±0.1		9
2012-02-13	55971	16.65±0.1		9
2012-02-20	55978	16.35±0.1		9
2012-03-19	56006	16.15±0.1		9
2012-03-31	56018	16.35±0.1		9
2012-04-16	56034	16.0±0.1		9
2012-04-27	56045	16.5±0.1		9
2012-05-07	56055	16.15±0.1		9
2012-08-16	56155	16.4±0.1		9
2012-10-10	56211	16.75±0.1		9
2012-11-01	56232	16.55±0.1	13.98±0.1	9
2012-11-08	56239	16.7±0.1	14.1±0.1	9
2012-11-13	56245	16.6±0.1	14.08±0.1	9
2012-11-25	56257	16.45±0.1	14.09±0.1	9
2012-12-07	56268	16.6±0.1	14.2±0.1	9
2012-12-17	56279	16.7±0.1	14.14±0.1	9
2012-12-26	56287	16.45±0.1	14.21±0.1	9
2013-01-02	56295	16.65±0.1	14.22±0.1	9
2013-01-13	56306	16.65±0.1	14.19±0.1	9
2013-01-23	56316	16.8±0.1	14.21±0.1	9
2013-02-04	56328	16.7±0.1	14.28±0.1	9
2013-02-20	56344	16.8±0.1	14.22±0.1	9
2013-03-03	56355	16.75±0.1	14.2±0.1	9
2013-03-20	56372	16.5±0.1	14.25±0.1	9
2013-04-06	56389	16.6±0.1	14.2±0.1	9
2013-05-05	56418	16.6±0.1	14.08±0.1	9
2013-06-06	56449	16.35±0.1	14.19±0.1	9
2013-06-06	56449	15.75±0.30		10
2013-07-07	56480	16.6±0.1	14.4±0.1	9
2013-07-30	56503	16.75±0.1	14.63±0.1	9
2013-09-01	56536	16.8±0.1	14.95±0.1	9
2013-09-13	56548	17.1±0.1	14.98±0.1	9
2013-10-08	56573	16.85±0.1	15.13±0.1	9
2013-10-28	56594	16.85±0.1	15.1±0.1	9
2013-11-21	56618	16.8±0.1	15.22±0.1	9
2013-12-05	56632	17.15±0.1	15.15±0.1	9
2013-12-18	56645	17.25±0.1	15.12±0.1	9
2013-12-26	56653	17.1±0.1	15.16±0.1	9
2014-01-11	56669	17.3±0.1	15.32±0.1	9
2014-01-31	56689	17.15±0.1	15.25±0.1	9
2014-02-21	56710	17.25±0.1	15.15±0.1	9
2014-03-05	56722	17.05±0.1	15.22±0.1	9
2014-03-21	56738	17.0±0.1	15.1±0.1	9

2014-03-27	56744		17.0±0.1	14.96±0.1	9
2014-04-05	56753		16.9±0.1	14.97±0.1	9
2014-04-16	56764		16.8±0.1	14.86±0.1	9
2014-04-24	56772		16.9±0.1	14.85±0.1	9
2014-05-01	56779		16.7±0.1	14.71±0.1	9
2014-05-09	56787		16.8±0.1	14.74±0.1	9
2014-05-18	56796		16.4±0.1	14.68±0.1	9
2014-05-28	56806			14.51±0.1	9
2014-05-30	56808		16.5±0.1	14.46±0.1	9
2014-06-11	56820			14.56±0.1	9
2014-06-17	56825		16.25±0.1	14.44±0.1	9
2014-06-28	56836		16.32±0.1	14.54±0.1	9
2014-07-08	56846		16.55±0.1	14.56±0.1	9
2014-07-21	56859		16.25±0.1	14.46±0.1	9
2014-08-16	56885		16.15±0.1	14.48±0.1	9
2014-08-27	56896		15.92±0.1	14.28±0.1	9
2014-09-13	56913		16.02±0.1	14.38±0.1	9
2014-09-21	56921		16.18±0.1	14.36±0.1	9
2014-10-05	56935		16.2±0.1	14.29±0.1	9
2014-10-18	56948		16.05±0.1	14.25±0.1	9
2014-11-14	56975		16.3±0.1	14.36±0.1	9
2014-11-26	56987		16.65±0.1	14.33±0.1	9
2014-12-15	57007		16.16±0.1	14.29±0.1	9
2015-01-07	57030		16.25±0.1	14.33±0.1	9
2015-01-09	57032		16.4±0.1	14.31±0.1	9
2015-01-29	57051		16.35±0.1	14.33±0.1	9
2015-02-16	57070		16.34±0.1	14.46±0.1	9
2015-02-27	57081		16.47±0.1	14.47±0.1	9
2015-03-18	57100		16.49±0.1	14.49±0.1	9
2015-03-28	57110		16.52±0.1	14.55±0.1	9
2015-04-07	57120		16.57±0.1	14.49±0.1	9
2015-04-23	57136		16.62±0.1	14.56±0.1	9
2015-05-06	57149		16.5±0.1	14.58±0.1	9
2015-05-16	57159		16.5±0.1	14.56±0.1	9
2015-05-25	57168		16.33±0.1	14.45±0.1	9
2015-07-08	57211	16.46±0.07	16.31±0.06		11
2015-07-15	57218		16.2±0.1	14.37±0.1	9
2015-07-29	57232		16.437±0.113		12
2015-08-04	57239	16.842±0.120	16.383±0.063		12
2015-08-10	57245	16.929±0.090	16.203±0.073		12
2015-08-20	57255	17.733±0.183	16.185±0.073		12
2015-08-22	57256		16.4±0.1	14.25±0.1	9
2015-08-25	57260	17.083±0.098	16.104±0.060		12
2015-09-06	57272	16.777±0.084	16.400±0.064		12
2015-09-04	57269		16.06±0.1	14.2±0.1	9
2015-09-13	57278		16.22±0.1	14.14±0.1	9
2015-09-21	57286		16.27±0.1	14.37±0.1	9
2015-10-06	57301		16.56±0.1	14.27±0.1	9
2015-10-13	57308		16.51±0.1	14.32±0.1	9
2015-10-28	57323		16.47±0.1	14.35±0.1	9
2015-11-06	57333		16.5±0.1	14.42±0.1	9
2015-11-09	57336	16.876±0.062	16.336±0.025		12
2015-11-12	57339	16.761±0.039	16.276±0.026		12
2015-11-12	57339		16.249±0.021	16.719±0.071	12
2015-11-16	57343		16.258±0.028		12
2015-11-16	57343		16.25±0.1	14.39±0.1	9
2015-11-18	57344	16.711±0.027	16.368±0.033		12
2015-11-22	57349	16.820±0.105			12
2015-11-25	57352	16.764±0.086	16.195±0.032		12
2015-11-27	57354	16.730±0.110	16.317±0.039		12
2015-11-24	57350			14.52±0.1	9
2015-12-03	57360		16.42±0.1	14.44±0.1	9
2015-12-14	57371		16.61±0.1	14.49±0.1	9
2015-12-17	57374		16.45±0.1	14.47±0.1	9

2015-12-26	57383	16.821±0.066	16.307±0.043		12
2015-12-27	57384		16.47±0.1	14.46±0.1	9
2016-01-06	57393		16.8±0.1	14.43±0.1	9
2016-01-08	57396		16.35±0.1	14.41±0.1	9
2016-01-19	57407		16.33±0.1	14.4±0.1	9
2016-01-27	57415		16.48±0.1	14.41±0.1	9
2016-01-31	57419	16.960±0.033	16.216±0.028		12
2016-01-31	57419		16.4±0.1	14.44±0.1	9
2016-02-08	57427		16.35±0.1	14.38±0.1	9
2016-02-09	57428		16.4±0.1	14.33±0.1	9
2016-02-14	57433		16.25±0.1	14.39±0.1	9
2016-02-16	57435		16.23±0.1	14.31±0.1	9
2016-02-20	57439	16.745±0.074	16.313±0.037		12
2016-02-23	57442		16.21±0.1	14.34±0.1	9
2016-02-27	57446		16.39±0.1	14.31±0.1	9
2016-03-04	57452		16.25±0.1	14.33±0.1	9
2016-03-09	57457		16.35±0.1	14.37±0.1	9
2016-03-11	57459		16.52±0.1	14.37±0.1	9
2016-03-14	57462		16.35±0.1	14.43±0.1	9
2016-03-16	57464		16.32±0.1	14.32±0.1	9
2016-03-17	57465	16.721±0.038	16.203±0.025		12
2016-03-22	57470	16.792±0.064	16.524±0.117		12
2016-03-26	57474		16.27±0.1	14.39±0.1	9
2016-03-28	57476		16.62±0.1	14.37±0.1	9
2016-04-01	57480		16.77±0.1	14.49±0.1	9
2016-04-03	57482		16.45±0.1	14.49±0.1	9
2016-04-06	57485		16.5±0.1	14.5±0.1	9
2016-04-07	57486		16.46±0.1	14.53±0.1	9
2016-04-10	57489		16.41±0.1	14.59±0.1	9
2016-04-14	57493		16.35±0.1	14.5±0.1	9
2016-04-23	57502		16.3±0.1	14.75±0.1	9
2016-04-28	57507		16.37±0.1	14.72±0.1	9
2016-04-30	57509		16.92±0.1	14.7±0.1	9
2016-05-04	57513		16.9±0.1	14.67±0.1	9
2016-05-10	57519		16.72±0.1	14.64±0.1	9
2016-05-14	57523		16.42±0.1	14.67±0.1	9
2016-05-20	57529		16.7±0.1	14.73±0.1	9
2016-05-25	57534		16.83±0.1	14.82±0.1	9
2016-06-01	57541			14.88±0.1	9
2016-06-05	57545		16.54±0.1	14.81±0.1	9
2016-06-08	57548		16.86±0.1	14.75±0.1	9
2016-06-16	57556		16.63±0.1	14.82±0.1	9
2016-06-21	57561			14.9±0.1	9
2016-06-28	57568			14.92±0.1	9
2016-08-01	57601		16.75±0.1	14.83±0.1	9
2016-08-11	57611		17.07±0.1	14.88±0.1	9
2016-08-27	57627		16.6±0.1	14.85±0.1	9
2016-09-12	57643		16.7±0.1	14.84±0.1	9
2016-09-22	57654	17.010±0.042	16.578±0.032		12
2016-09-24	57655		16.93±0.1	14.79±0.1	9
2016-10-02	57664	16.602±0.084	16.305±0.068		12
2016-10-11	57672		17.05±0.1	14.83±0.1	9
2016-10-12	57674	17.089±0.080	17.313±0.270		12
2016-10-13	57675		16.88±0.1	14.71±0.1	9
2016-10-20	57682		16.5±0.1	14.64±0.1	9
2016-10-23	57685		16.63±0.1	14.73±0.1	9
2016-10-25	57687		16.66±0.1	14.65±0.1	9
2016-10-30	57692		16.79±0.1	14.66±0.1	9
2016-11-06	57699		16.72±0.1	14.7±0.1	9
2016-11-18	57711		16.52±0.1	14.76±0.1	9
2016-11-25	57718		16.71±0.1	14.7±0.1	9
2016-11-30	57722		16.66±0.1	14.82±0.1	9
2016-12-01	57724		16.62±0.1	14.76±0.1	9
2016-12-08	57730		17.05±0.1	14.79±0.1	9

2016-12-11	57734	16.58±0.1	14.82±0.1	9
2016-12-18	57741	16.59±0.1	14.81±0.1	9
2016-12-25	57748	16.57±0.1	14.86±0.1	9
2016-12-29	57752	17.02±0.1	14.88±0.1	9
2017-01-04	57758	16.71±0.1	14.95±0.1	9
2017-01-10	57764	16.69±0.1		9
2017-01-11	57765	16.52±0.1	14.89±0.1	9
2017-01-17	57771	16.68±0.1	14.97±0.1	9
2017-01-28	57782	16.71±0.1	15.0±0.1	9
2017-02-03	57788	16.77±0.1	15.0±0.1	9
2017-02-06	57791	16.54±0.1	14.97±0.1	9
2017-02-15	57800	16.7±0.1	14.88±0.1	9
2017-02-17	57802	16.78±0.1	14.92±0.1	9
2017-02-21	57806	16.62±0.1	14.92±0.1	9
2017-03-05	57818	16.64±0.1	14.76±0.1	9
2017-03-06	57819	16.62±0.1	14.78±0.1	9
2017-03-13	57826	16.59±0.1	14.82±0.1	9
2017-03-16	57829	16.57±0.1	14.78±0.1	9
2017-03-21	57834	16.95±0.1	14.64±0.1	9
2017-03-25	57838	16.55±0.1	14.66±0.1	9
2017-03-26	57839	16.54±0.1	14.73±0.1	9
2017-03-29	57842	16.55±0.1	14.69±0.1	9
2017-04-02	57846	16.69±0.1	14.74±0.1	9
2017-04-09	57853	16.57±0.1	14.67±0.1	9
2017-04-11	57855	16.51±0.1	14.61±0.1	9
2017-04-15	57859	16.5±0.1	14.6±0.1	9
2017-04-17	57861	16.53±0.1	14.61±0.1	9
2017-04-21	57865	16.42±0.1	14.56±0.1	9
2017-04-27	57871	16.54±0.1	14.66±0.1	9
2017-05-02	57876	16.57±0.1	14.62±0.1	9
2017-05-04	57878	16.61±0.1	14.62±0.1	9
2017-05-09	57883	16.64±0.1	14.59±0.1	9
2017-05-12	57886	16.83±0.1	14.56±0.1	9
2017-05-19	57893	16.62±0.1	14.65±0.1	9
2017-05-28	57902	16.74±0.1	14.65±0.1	9
2017-06-02	57907		14.62±0.1	9
2017-07-12	57946	16.9±0.1	14.7±0.1	9
2017-07-18	57952		14.76±0.1	9
2017-07-19	57953	17.1±0.1	14.68±0.1	9
2017-07-24	57958		14.74±0.1	9
2017-08-14	57979	16.57±0.1	14.7±0.1	9
2017-08-23	57988	16.58±0.1	14.6±0.1	9
2017-08-30	57996	16.72±0.1	14.82±0.1	9
2017-09-02	57998	16.69±0.1	14.76±0.1	9
2017-09-21	58017		14.53±0.1	9
2017-09-24	58021		14.67±0.1	9
2017-10-13	58040	16.85±0.1	14.68±0.1	9
2017-10-23	58050	17.12±0.1	14.7±0.1	9
2017-10-27	58054	16.8±0.1	14.76±0.1	9
2017-11-06	58064	16.78±0.1	14.66±0.1	9
2017-11-16	58074	16.83±0.1	14.56±0.1	9
2017-11-24	58082	16.84±0.1	14.62±0.1	9
2017-12-07	58095	16.76±0.1	14.54±0.1	9
2017-12-11	58098		14.62±0.1	9
2017-12-14	58102	16.92±0.1	14.53±0.1	9
2017-12-19	58107	16.77±0.1	14.52±0.1	9
2017-12-20	58108	16.94±0.1	14.59±0.1	9
2017-12-25	58113	16.83±0.1	14.58±0.1	9
2017-12-26	58114	16.73±0.1	14.56±0.1	9
2017-12-28	58116	16.98±0.1	14.61±0.1	9
2017-12-30	58118	16.8±0.1	14.52±0.1	9
2018-01-01	58120	16.76±0.1	14.52±0.1	9
2018-01-04	58123	16.75±0.1	14.44±0.1	9
2018-01-06	58125	16.73±0.1	14.53±0.1	9

2018-01-09	58128	16.82±0.1	14.49±0.1	9
2018-01-11	58130	16.59±0.1	14.51±0.1	9
2018-01-12	58131		14.53±0.1	9
2018-01-13	58132	16.6±0.1	14.47±0.1	9
2018-01-16	58135		14.47±0.1	9
2018-01-17	58136		14.46±0.1	9
2018-01-28	58147	16.71±0.1	14.4±0.1	9
2018-02-01	58151	16.68±0.1	14.42±0.1	9
2018-02-04	58154	16.65±0.1	14.38±0.1	9
2018-02-05	58155		14.44±0.1	9
2018-02-07	58157		14.4±0.1	9
2018-02-09	58159		14.37±0.1	9
2018-02-14	58164	16.75±0.1	14.32±0.1	9
2018-02-19	58169	16.74±0.1	14.34±0.1	9
2018-02-22	58172		14.33±0.1	9
2018-02-25	58175	16.66±0.1	14.32±0.1	9
2018-03-03	58181		14.22±0.1	9
2018-03-11	58189	16.51±0.1	14.22±0.1	9
2018-03-17	58195		14.25±0.1	9
2018-03-20	58198	16.47±0.1	14.21±0.1	9
2018-03-22	58200	16.42±0.1	14.2±0.1	9
2018-03-23	58201		14.19±0.1	9
2018-03-26	58204	16.44±0.1	14.24±0.1	9
2018-04-01	58210	16.53±0.1	14.19±0.1	9
2018-04-06	58215	16.46±0.1	14.19±0.1	9
2018-04-11	58220	16.45±0.1	14.1±0.1	9
2018-04-12	58221		14.16±0.1	9
2018-04-15	58224	16.43±0.1	14.18±0.1	9
2018-04-17	58226	16.55±0.1	14.15±0.1	9
2018-04-20	58229	16.56±0.1	14.1±0.1	9
2018-04-26	58235	16.35±0.1	14.12±0.1	9
2018-05-03	58242	16.5±0.1	14.14±0.1	9
2018-05-09	58248	16.41±0.1	14.11±0.1	9

References. (1): SuperCOSMOS Sky Surveys (Hambly et al. 2001); (2): The HST Guide Star Catalog, Version 1.2 (Morrison et al. 2001); (3): The USNO-A2.0 Catalogue (Monet et al. 1992); (4): The USNO-B1.0 Catalog (Monet et al. 2003); (5): Remillard et al. (1992); (6): Muerse et al. (1996); (7): DENIS Catalogue toward Magellanic Clouds (Cioni et al. 2000); (8): 2MASS All-Sky Catalog of Point Sources (Skrutskie et al. 2006); (9): INTEGRAL OMC (Giménez et al. 2001); (10): This work (Kleinkaroo Observatory); (11): This work (Du Pont); (12) Observations of Bart Staels from the American Association of Variable Star Observers (AAVSO). AAVSO UID=000-BCZ-119

Table A.2. Swift UV observations of LMC S154.

Date	Exposure [s]	UVM2 [mag]
2014-05-17	383	16.94 ± 0.07
2014-10-08	234	16.43 ± 0.07
2014-10-09	454	16.46 ± 0.05
2014-10-10	462	16.37 ± 0.05
2014-10-25	164	16.60 ± 0.09
2014-11-28	360	16.39 ± 0.06
2014-12-05	410	16.35 ± 0.05
2014-12-30	169	16.41 ± 0.08
2015-01-01	132	16.42 ± 0.09
2015-01-06	581	16.43 ± 0.05
2015-01-19	479	16.42 ± 0.05
2015-01-22	152	16.41 ± 0.08
2015-01-24	613	16.32 ± 0.04
2015-01-26	242	16.57 ± 0.07
2015-01-27	190	16.33 ± 0.07
2015-05-05	509	16.41 ± 0.05
2015-05-07	449	16.36 ± 0.05
2015-05-10	745	16.35 ± 0.04
2015-05-12	494	16.45 ± 0.05
2015-06-16	159	16.16 ± 0.07
2015-06-27	845	16.22 ± 0.04
2015-07-01	200	16.24 ± 0.07
2015-10-08	325	16.18 ± 0.06
2015-10-09	679	16.09 ± 0.04
2015-10-11	352	16.03 ± 0.05
2015-11-06	130	16.09 ± 0.08
2015-11-08	130	16.09 ± 0.08
2015-11-19	444	16.10 ± 0.05
2015-12-04	773	16.10 ± 0.04
2016-07-25	290	16.13 ± 0.06
2016-07-26	795	16.19 ± 0.04
2016-07-27	1094	16.21 ± 0.04
2016-07-28	895	16.21 ± 0.04
2016-07-29	1596	16.23 ± 0.03
2016-07-31	203	16.18 ± 0.07